

Dark and visible matter distribution in Coma cluster: theory vs observations

Ruslan Brilenkov¹, Maxim Eingorn² and Alexander Zhuk³

¹Department of Theoretical Physics, Odessa National University,
Dvoryanskaya st. 2, Odessa 65082, Ukraine

²North Carolina Central University, CREST and NASA Research Centers,
Fayetteville st. 1801, Durham, North Carolina 27707, U.S.A.

³Astronomical Observatory, Odessa National University,
Dvoryanskaya st. 2, Odessa 65082, Ukraine

E-mail: ruslan.brilenkov@gmail.com, maxim.eingorn@gmail.com,
ai.zhuk2@gmail.com

Abstract. We investigate dark and visible matter distribution in the Coma cluster in the case of the Navarro-Frenk-White (NFW) profile. A toy model where all galaxies in the cluster are concentrated inside a sphere of an effective radius R_{eff} is considered. It enables to obtain the mean velocity dispersion as a function of R_{eff} . We show that, within the observation accuracy of the NFW parameters, the calculated value of R_{eff} can be rather close to the observable cutoff of the galaxy distribution. Moreover, the comparison of our toy model with the observable data and simulations leads to the following preferable NFW parameters for the Coma cluster: $R_{200} \approx 1.77 h^{-1} \text{ Mpc} = 2.61 \text{ Mpc}$, $c = 3 \div 4$ and $M_{200} = 1.29 h^{-1} \times 10^{15} M_{\odot}$. In the Coma cluster the most of galaxies are concentrated inside a sphere of the effective radius $R_{eff} \sim 3.7 \text{ Mpc}$ and the line-of-sight velocity dispersion is 1004 km s^{-1} .

Contents

1	Introduction	1
2	Zero acceleration sphere and mean velocity dispersion	2
3	Navarro-Frenk-White profile in the Coma cluster. Theory vs observations and simulations	5
4	Conclusion	9

1 Introduction

According to the recent observations [1–5], our Universe is dark: dark energy and dark matter contribute approximately 69% and 26% into total mass-energy balance in the Universe, respectively. Different independent observations also indicate that dark matter (DM) envelops the galaxies and clusters of galaxies. Baryonic matter is only 10-15% of the total mass of clusters of galaxies [6]. The rest is DM. Unfortunately, the nature of DM (as well as dark energy) is still unclear and is a subject of numerous investigations [7]. The standard cosmological model, i.e. the Λ CDM model, assumes that DM is cold. This model is rather successful in explaining the structure formation in the Universe. There is a quite big number of papers devoted to the investigations (analytical and numerical) of the structure and dynamics of galaxies and clusters of galaxies (see, e.g., the reviews [8] and [9]). For these investigations, the spherical density profile $\rho(R)$ of DM in galaxies and clusters of galaxies is very useful. On the one hand, such profiles help to reveal different universal scaling relations [10–12]. On the other hand, they help to study the observable properties of DM in halos of galaxies and clusters of galaxies [6, 13, 14] and are used in the recent numerical simulations [15]. These profiles also represent a very useful tool for modeling the mass distribution in halos [16] as well as for analytical analysis of properties of DM halos [17].

Galaxies, groups and clusters of galaxies are the inhomogeneities we observe inside the cell of uniformity which is of the order of 190 Mpc [18]. Deep inside this cell, the Universe is highly inhomogeneous and is well described by the discrete cosmology approach [18, 19]. The structure and dynamics of inhomogeneities are influenced by two main factors. They are the gravitational attraction between the constituents of these objects and the cosmological expansion of the Universe. Obviously, there is a distance from the center of mass of an inhomogeneity at which the cosmological expansion begins to prevail over the gravitational attraction. Moreover, because the expansion in the late Universe is accelerating, both of these phenomena act against each other. This means that the corresponding forces are directed oppositely. This effect was observed experimentally [20–23] and the corresponding distance was called the radius of the zero velocity surface. In [24] this distance has received the name of the radius of zero gravity. In our opinion, this distance is more properly termed as the radius of the zero acceleration [18, 19] because gravity does not disappear at this distance but the acceleration of a test body (a dwarf galaxy) is equal (or approximately equal) to zero. This distance for the Local Group was estimated in [25].

It is natural to suppose that the edge of the DM halo in clusters of galaxies corresponds to the surface of the zero acceleration. This idea was discussed in [17]. Here, the authors

considered the background metric in the form of the Schwarzschild-de Sitter (SdS) solution. Such approach disregards the presence of matter in the Universe. However, in the Λ CDM model matter contributes 31% into the total mass-energy balance. Therefore, in the present paper we include matter into account considering the Friedmann-Robertson-Walker (FRW) metric as the background one.

In section 2, we start from the investigation of the gravitational potential produced by a spherically distributed DM halo. This potential satisfies the Poisson equation [19]. We supplement this equation with the proper boundary conditions at the surface of zero acceleration. Then, with the help of the virial theorem, we define the mean velocity dispersion of the galaxies which we consider as test bodies in the cluster DM halo. Here we use the observation [26] that distribution of galaxies in rich clusters is abruptly bounded at some distances much smaller than the size of a cluster. Thus, we introduce an effective radius R_{eff} and suppose that all galaxies are concentrated inside a sphere of this radius. In section 3, we apply the derived formulae to the case of the Navarro-Frenk-White (NFW) DM profile for the Coma cluster. Here, first, we demonstrate that R_{eff} is close to the observable value if we use the NFW profile parameters for the Coma cluster found from the observations and simulations. Second, the comparison of our toy model with the observable data and simulations enables us to get preferable NFW profile parameters for the Coma cluster. The main results are briefly summarized in concluding section 4.

2 Zero acceleration sphere and mean velocity dispersion

In the framework of discrete cosmology developed in the recent series of papers [18, 19, 25] the acceleration of any test body in the gravitational field of a spherically symmetric gravitationally bound system is given by the formula (see, e.g., section 4 in [19])

$$\ddot{R} = \frac{\ddot{a}}{a}R - \frac{\partial\Phi}{\partial R}, \quad (2.1)$$

where R is the distance from the center of mass of the system to a test body, a is the scale factor of the Universe, the overdots denote the derivatives with respect to the synchronous time, and the gravitational potential Φ satisfies the Poisson equation

$$\Delta\Phi = \frac{1}{R} \frac{d^2}{dR^2}(R\Phi) = 4\pi G_N \rho_{ph}, \quad (2.2)$$

where G_N is the Newtonian gravitational constant and ρ_{ph} is the physical (not comoving!) rest mass density of the bound system. It is worth noting that Eq. (2.1) was obtained in [19] for the Universe with hyperbolic spatial topology $\mathcal{K} = -1$. However, deep inside the cell of uniformity (with the size of the order of 190 Mpc [18]) the Universe can be considered with very high accuracy as spatially flat. Therefore, we can drop the contribution of \mathcal{K} to (2.2) and consider the Laplace operator Δ in cartesian (physical) coordinates. It should be mentioned that in the Newtonian limit the similar equations (of the form (2.1) and (2.2)) were obtained in [27] and are used for the N-body simulations [28].

The term $(\ddot{a}/a)R$ in (2.1) arises due to the global cosmological expansion of the Universe while the term with $\Phi(R)$ takes into account the gravitational attraction between a test body and the gravitationally bound system. According to the recent observations, our present Universe undergoes the stage of the accelerated expansion. For the Λ CDM model, this stage

started at the redshift $z \approx 0.76$ [29]. It means that from this time $\ddot{a} > 0$. Therefore, Eq. (2.1) demonstrates that (starting from this time) there is a distance R_H from the center of mass of the system at which the gravitational attraction and the cosmological expansion compensate each other:

$$\ddot{R}\Big|_{R_H} = 0 \quad \Rightarrow \quad R_H = \frac{\partial\Phi/\partial R}{\ddot{a}/a}\Big|_{R_H}. \quad (2.3)$$

Obviously, the Hubble flows begin to form at distances greater than R_H . We can also rewrite Eq. (2.1) in the form

$$\ddot{R} = -\frac{\partial\tilde{\Phi}}{\partial R}, \quad (2.4)$$

where

$$\tilde{\Phi}(R) = -\frac{1}{2}\frac{\ddot{a}}{a}R^2 + \Phi(R). \quad (2.5)$$

Then, the zero acceleration condition is

$$\frac{\partial\tilde{\Phi}}{\partial R}\Big|_{R_H} = 0. \quad (2.6)$$

In the present paper, we consider gravitationally bound systems consisting of a rather large number of inhomogeneities/galaxies which have a common (for a whole system) DM haloes. DM halos make a dominant contribution to the total mass of the systems and galaxies are considered as test bodies. Such situation takes place in rich clusters of galaxies, e.g., for the Virgo cluster which consists of about 2000 galaxies [23, 30]. It is well known that the shape of this cluster is rather far from spherically symmetric [31, 32]. The cluster is an aggregate of at least three separate subclumps. In general, there is no problem to define a surface (or an approximate surface) of zero acceleration in the case of a number of gravitating sources which make the dominant contributions to the gravitational acceleration [25]. However, the DM profiles for galaxies and clusters of galaxies are usually modeled by the spherically symmetric distributions of DM. The Coma cluster (Abell 1656) has more spherical distribution¹. Therefore, in what follows we consider the Coma cluster which, in a rough approximation, has an overall DM halo of the spherically symmetric form.

It is natural to suppose that the edge/cutoff of a DM halo coincides with the surface of zero acceleration. DM particles are confined by the gravitational interaction inside the domain bounded by this surface and are “blown” by the cosmological expansion outside it. According to the observations, DM makes the main contribution into the mass of galaxies, groups and clusters of galaxies. Then, the rest mass density ρ_{ph} in Eq. (2.2) is mainly defined by DM. For simplicity neglecting the contribution of the visible matter as compared with that of DM, for the halo mass we obtain

$$M = 4\pi \int_0^{R_H} \rho_{\text{ph}}(R) R^2 dR. \quad (2.7)$$

It is clear that the gravitational potential Φ should satisfy the following boundary condition: $\Phi \rightarrow -G_N M/R_H$ for $R \rightarrow R_H$. Therefore, the boundary conditions for the potential $\tilde{\Phi}$ are:

$$\frac{d\tilde{\Phi}}{dR}\Big|_{R=R_H} = 0, \quad \tilde{\Phi}(R_H) = -\frac{1}{2}\frac{\ddot{a}}{a}R_H^2 - \frac{G_N M}{R_H}. \quad (2.8)$$

¹Although here we also observe subhalos [33].

For the given above boundary conditions, the radius of the zero acceleration sphere is

$$R_H = \left[\frac{G_N M}{\ddot{a}/a} \right]^{1/3} \Rightarrow \tilde{\Phi}(R_H) = -\frac{3}{2} \frac{G_N M}{R_H}. \quad (2.9)$$

Obviously, the value of R_H depends on time. On the other hand, Eq. (2.9) results in a useful relation

$$\frac{\ddot{a}}{a} R_H^3 = G_N M. \quad (2.10)$$

The ratio \ddot{a}/a can be obtained from the second Friedmann equation. In the case of the Λ CDM model we have:

$$\frac{\ddot{a}}{a} = -\frac{\kappa \bar{\rho} c^4}{6a^3} + \frac{\Lambda c^2}{3} = H_0^2 \left(-\frac{1}{2} \Omega_M \frac{a_0^3}{a^3} + \Omega_\Lambda \right) > 0, \quad (2.11)$$

where $\kappa = 8\pi G_N/c^4$ (with c being the speed of light) and we took into account the late time acceleration of the Universe expansion. In accordance with the conventional Λ CDM model, the Universe is supposed to be filled with the nonrelativistic matter (dust) characterized by the average rest mass density $\bar{\rho}$ (being constant in the comoving reference frame) and the dark energy represented by the cosmological constant Λ . We also introduce the standard density parameters

$$\Omega_M = \frac{\kappa \bar{\rho} c^4}{3H_0^2 a_0^3}, \quad \Omega_\Lambda = \frac{\Lambda c^2}{3H_0^2}, \quad (2.12)$$

where a_0 and H_0 are the current values of the scale factor and the Hubble parameter $H(t) = \dot{a}/a$, respectively. Therefore, from (2.9) we get

$$R_H = \frac{(G_N M)^{1/3}}{\left[H_0^2 \left(-\frac{1}{2} \Omega_M \frac{a_0^3}{a^3} + \Omega_\Lambda \right) \right]^{1/3}}. \quad (2.13)$$

If instead of the discrete cosmology approach the Schwarzschild-de Sitter one is applied (see, e.g., [17]), then in the above and following formulae we should simply put $\Omega_M \equiv 0$, thus disregarding the contribution of matter. However, according to the recent observations, matter contributes approximately 30% into the total balance (dark energy/ Λ -term gives another 70%). Hence, dropping the contribution of matter corresponds to a decrease in accuracy of 30 percent. At the present, we are entering the era of precision cosmology. Therefore, future observations can reveal these discrepancies.

The mean velocity dispersion of galaxies σ in clusters is one of their important observable parameters [34]. With respect to the Coma cluster, the line-of-sight velocity dispersion is $954 \pm 50 \text{ km s}^{-1}$ [26] (the authors of [34] obtained a bit different value of $\sigma \approx 1008 \text{ km s}^{-1}$). We can estimate σ with the help of the virial theorem. Eq. (2.4) can be written in the form

$$\dot{\mathbf{V}} = -\frac{\partial \tilde{\Phi}}{\partial R} \frac{\mathbf{R}}{R}, \quad (2.14)$$

Multiplying both sides of Eq. (2.14) by \mathbf{R} , one gets:

$$\frac{d}{dt}(\mathbf{V}\mathbf{R}) = V^2 - \frac{\partial \tilde{\Phi}}{\partial R} R. \quad (2.15)$$

Because V and R are finite functions, averaging this equation over times which are much longer than characteristic periods of the system, we can eliminate the left hand side of (2.15). Next, we average over the volume of the halo and obtain

$$\overline{V^2} = \overline{\frac{\partial \tilde{\Phi}}{\partial R} R}. \quad (2.16)$$

The mean velocity dispersion $\sigma = (\overline{V^2})^{1/2}$. If the number density of galaxies over the entire volume of the halo (i.e. for $R \in [0, R_H]$) is constant, then

$$\overline{V^2} = \frac{4\pi}{V_H} \int_0^{R_H} \frac{\partial \tilde{\Phi}}{\partial R} R^3 dR, \quad V_H = \frac{4}{3}\pi R_H^3. \quad (2.17)$$

However, observations indicate that distribution of galaxies is abruptly bounded at some distance R_{2t} which is considerably less than the size of the cluster. The most galaxies are inside this distance from the center of mass of the Coma cluster [26]. Therefore, the averaging over the entire volume of the halo gives the wrong result. Unfortunately, we do not know the real 3D picture for vectors of velocities \mathbf{V} of all galaxies in the Coma cluster. Hence, to get the mean velocity dispersion we need to introduce some theoretical model. Let us suppose a toy model where all galaxies are concentrated inside a sphere of the radius R_{eff} with the constant number density. There are no galaxies outside this sphere. For such picture,

$$\overline{V^2} = \frac{4\pi}{V_{eff}} \int_0^{R_{eff}} \frac{\partial \tilde{\Phi}}{\partial R} R^3 dR, \quad V_{eff} = \frac{4}{3}\pi R_{eff}^3. \quad (2.18)$$

Now we want to take a definite DM halo profile and, first, calculate the gravitational potential $\tilde{\Phi}$, second, obtain the mean velocity dispersion from the formula (2.18) as a function of R_{eff} . As we know the observable value of σ as well as the experimental values for the halo profile parameters, we can estimate unknown R_{eff} and compare it with the observable R_{2t} . If these two values are close to each other, it will demonstrate that our toy model determines more or less successfully the characteristic radius within which most of the galaxies are located. On the other hand, if R_{eff} is close to the observable value, we can use this model to determine parameters of the considered DM halo profile. In the next section, we demonstrate our approach on the example of the NFW profile.

3 Navarro-Frenk-White profile in the Coma cluster. Theory vs observations and simulations

At the present, the NFW profile [35] is one of the most commonly used profiles to describe DM distribution in galaxies and clusters of galaxies. It reads

$$\rho_{ph}(R) = \frac{4\rho_s}{\frac{R}{R_s} \left(1 + \frac{R}{R_s}\right)^2}, \quad (3.1)$$

where $\rho_s = \rho_{ph}(R_s)$ and the scale radius R_s are free parameters of the profile. Since DM gives the main contribution to the total mass of the system, the mass M_* within a sphere of the radius R_* is

$$M_* \equiv M(R_*) = 16\pi\rho_s R_s^3 \left[\ln \left(1 + \frac{R_*}{R_s}\right) - \frac{R_*}{R_s + R_*} \right]. \quad (3.2)$$

Then, the total mass of the cluster is $M \equiv M(R_H)$. Very often DM profiles are characterized by the mass $M_{200} \equiv M(R_{200})$ where the radius R_{200} defines a sphere where the average DM density $\bar{\rho}_{200}$ equals 200 ρ_{crit} with

$$\rho_{crit} = 3H_0^2/(8\pi G_N) \approx 1.88 h^2 \times 10^{-26} \text{ kg m}^{-3} \quad (3.3)$$

being the critical density of the Universe today. According to the most recent Planck results [5], $\Omega_M \approx 0.3$ and $\Omega_\Lambda \approx 0.7$. Besides, $H_0 \approx 67.8 \text{ km s}^{-1} \text{ Mpc}^{-1}$, therefore, $h \approx 0.678$. Hence, by the definition

$$M_{200} = \frac{4}{3}\pi R_{200}^3 \bar{\rho}_{200}, \quad \bar{\rho}_{200} = 200\rho_{crit}. \quad (3.4)$$

It follows from Eq. (2.13) that the total mass

$$M = \frac{8\pi}{3}\rho_{crit}R_H^3 \left(-\frac{1}{2}\Omega_M + \Omega_\Lambda\right) = \frac{M_{200}}{100} \left(\frac{\lambda_H}{c}\right)^3 \left(-\frac{1}{2}\Omega_M + \Omega_\Lambda\right), \quad (3.5)$$

where

$$\lambda_H \equiv \frac{R_H}{R_s}, \quad c \equiv \frac{R_{200}}{R_s}. \quad (3.6)$$

The parameter c is usually called the concentration parameter. On the other hand, from Eq. (3.2) we have

$$M = M_{200} \frac{\ln(1 + \lambda_H) - \frac{\lambda_H}{1 + \lambda_H}}{\ln(1 + c) - \frac{c}{1 + c}}. \quad (3.7)$$

Equating (3.5) and (3.7), we get the following useful relation:

$$\frac{1}{100} \left(-\frac{1}{2}\Omega_M + \Omega_\Lambda\right) \frac{1}{c^3} \left[\ln(1 + c) - \frac{c}{1 + c}\right] = \frac{1}{\lambda_H^3} \left[\ln(1 + \lambda_H) - \frac{\lambda_H}{1 + \lambda_H}\right]. \quad (3.8)$$

The ranges of parameters for the Coma cluster halo according to the observations are² [36]:

$$\begin{aligned} R_{200}^{(min)} &= 1.77 h^{-1} \text{ Mpc} = 2.61 \text{ Mpc}, & R_{200}^{(max)} &= 2.20 h^{-1} \text{ Mpc} = 3.24 \text{ Mpc}, \\ M_{200}^{(min)} &= 1.32 h^{-1} \times 10^{15} M_\odot, & M_{200}^{(max)} &= 2.53 h^{-1} \times 10^{15} M_\odot, \\ c_{min} &= 2, & c_{max} &= 17. \end{aligned} \quad (3.9)$$

Let us turn now to the gravitational potential and the velocity dispersion. To get the expression for the gravitational potential $\tilde{\Phi}$ defined in (2.5), we should first solve the Poisson equation (2.2) and, then, use the boundary conditions (2.8). As a result, we obtain:

$$\begin{aligned} \tilde{\Phi}(R) &= -\frac{\ddot{a}}{a} \left(\frac{R^2}{2} - R_H^2 + \frac{R_H^3}{R} \right) + 16\pi G_N \rho_s \frac{R_s^3}{R_s + R_H} \left(1 - \frac{R_H}{R} \right) \\ &- 16\pi G_N \rho_s \frac{R_s^3}{R} \ln \frac{R_s + R}{R_s + R_H} - \frac{G_N M}{R_H} = -\frac{G_N M}{R_H} \left\{ \frac{R^2}{2R_H^2} + \frac{R_H}{R} \right. \\ &+ \frac{R_H}{R} \frac{1}{\ln(1 + \lambda_H) - \frac{\lambda_H}{1 + \lambda_H}} \left[\frac{\lambda_H - R/R_s}{1 + \lambda_H} + \ln \frac{1 + R/R_s}{1 + \lambda_H} \right] \left. \right\}, \end{aligned} \quad (3.10)$$

²It is worth noting that if we calculate $M_{200}^{(min, max)}$ via the formula (3.4) with $R_{200}^{(min, max)}$ from (3.9), then we get a little bit different values: $M_{200}^{(min)} = 1.29 h^{-1} \times 10^{15} M_\odot$ and $M_{200}^{(max)} = 2.47 h^{-1} \times 10^{15} M_\odot$.

where for \ddot{a}/a we used Eq. (2.10) and ρ_s is expressed with the help of Eq. (3.2) for $R_* = R_H$. Now, we can calculate the velocity dispersion with the help of Eq. (2.18). Instead of $[\overline{V^2}]^{1/2}$, it makes sense to consider the dimensionless quantity $\tilde{\sigma}$:

$$\tilde{\sigma} = \left[\overline{V^2} \frac{R_H}{G_N M} \right]^{1/2} = \left(\frac{\lambda_H}{\lambda_{eff}} \right)^{1/2} \left[-\frac{3}{5} \left(\frac{\lambda_{eff}}{\lambda_H} \right)^3 + \frac{3}{2} + \frac{1}{\left[\ln(1 + \lambda_H) - \frac{\lambda_H}{1 + \lambda_H} \right]} \right. \\ \left. \times \left[\frac{3}{2} \frac{\lambda_H}{1 + \lambda_H} + \frac{9}{2} \frac{1}{\lambda_{eff}} - \frac{9}{4} - \frac{9}{2} \frac{1}{\lambda_{eff}^2} \ln(1 + \lambda_{eff}) + \frac{3}{2} \ln \frac{1 + \lambda_{eff}}{1 + \lambda_H} \right] \right]^{1/2}, \quad (3.11)$$

where

$$\lambda_{eff} \equiv \frac{R_{eff}}{R_s}. \quad (3.12)$$

On the other hand, from the definition of $\tilde{\sigma}$ we get

$$\tilde{\sigma} = \left[\overline{V^2} \frac{R_H}{G_N M} \right]^{1/2} = [\overline{V^2}]^{1/2} \left[\frac{3}{8\pi} \frac{c^2}{G_N \lambda_H^2 R_{200}^2 \rho_{crit}} \left(-\frac{1}{2} \Omega_M + \Omega_\Lambda \right)^{-1} \right]^{1/2}, \quad (3.13)$$

where R_H is expressed as $R_H = R_{200} \lambda_H / c$ and the total mass M is given by Eq. (3.5) with M_{200} from (3.4).

According to the observations [26], the line-of-sight velocity dispersion for the Coma cluster is $954 \pm 50 \text{ km s}^{-1}$. To get the 3D velocity dispersion we should multiply this value by $\sqrt{3}$. Therefore, the minimal and maximal 3D velocity dispersions are: $[\overline{(V^{(min)})^2}]^{1/2} = 1566 \text{ km s}^{-1}$ and $[\overline{(V^{(max)})^2}]^{1/2} = 1739 \text{ km s}^{-1}$, respectively. Therefore, the minimal and maximal values of $\tilde{\sigma}$ are:

$$\tilde{\sigma}^{(min)} = [\overline{(V^{(min)})^2}]^{1/2} \left[\frac{3}{8\pi} \frac{c^2}{G_N \lambda_H^2 (R_{200}^{(max)})^2 \rho_{crit}} \left(-\frac{1}{2} \Omega_M + \Omega_\Lambda \right)^{-1} \right]^{1/2}, \quad (3.14)$$

$$\tilde{\sigma}^{(max)} = [\overline{(V^{(max)})^2}]^{1/2} \left[\frac{3}{8\pi} \frac{c^2}{G_N \lambda_H^2 (R_{200}^{(min)})^2 \rho_{crit}} \left(-\frac{1}{2} \Omega_M + \Omega_\Lambda \right)^{-1} \right]^{1/2}, \quad (3.15)$$

where $R_{200}^{(min, max)}$ should be taken from (3.9).

According to Eq. (3.9), for the Coma cluster the concentration parameter $c \in [2, 17]$. Our task is to determine the values of R_{eff} as a function of c from this region. To perform it, we can start from $c = 2$ and then define R_{eff} for each value of c with the step, e.g., $\Delta c = 1$ up to $c = 17$. It is convenient to present the obtained values of R_{eff} in the corresponding table R_{eff} vs c . To demonstrate this procedure, let us consider as an example the case $c = 4$. For a given value of c , the parameter λ_H can be found from Eq. (3.8). In the considered example this is $\lambda_H = 33.28$. For this value of λ_H , the graph of $\tilde{\sigma}$ (see Eq. (3.11)) as a function of λ_{eff} is drawn in Fig. 1. From Eqs. (3.14) and (3.15), we can also get for $c = 4$: $\tilde{\sigma}^{(min)} = 1.15$ (lower horizontal line in Fig.1) and $\tilde{\sigma}^{(max)} = 1.60$ (upper horizontal line in Fig.1). It can be easily seen from this picture that for each value of $\tilde{\sigma}^{(min, max)}$ we have two roots. They are $\lambda_{eff,1} = 0.39$ and $\lambda_{eff,2} = 21.31$ for $\tilde{\sigma}^{(min)}$, $\lambda_{eff,3} = 1.58$ and $\lambda_{eff,4} = 5.68$ for $\tilde{\sigma}^{(max)}$. Since

$R_{eff,4}^{(min)}$	4.17	3.70	3.71	3.72	3.74	3.75	3.76	3.77
c	2	3	4	5	6	7	8	9
$R_{eff,4}^{(min)}$	3.78	3.78	3.79	3.80	3.80	3.80	3.81	3.81
c	10	11	12	13	14	15	16	17

Table 1. The values of the root $R_{eff,4}^{(min)}$ for different values of the concentration parameter c .

$\tilde{\sigma}^{(min)}$ ($\tilde{\sigma}^{(max)}$) was obtained with the help of $R_{200}^{(max)}$ ($R_{200}^{(min)}$), the corresponding values for $R_H = R_{200}\lambda_H/c$ and $R_s = R_{200}/c$ are $R_H^{(max)} = 26.99$ Mpc and $R_s^{(max)} = 0.81$ Mpc ($R_H^{(min)} = 21.72$ Mpc and $R_s^{(min)} = 0.65$ Mpc). Therefore, from the relation $R_{eff} = \lambda_{eff}R_s$ we obtain four marginal values: $R_{eff,1}^{(max)} = 0.32$ Mpc and $R_{eff,2}^{(max)} = 17.28$ Mpc (for $R_s^{(max)}$ and $\lambda_{eff1,2}$, correspondingly) and $R_{eff,3}^{(min)} = 1.03$ Mpc and $R_{eff,4}^{(min)} = 3.71$ Mpc (for $R_s^{(min)}$ and $\lambda_{eff3,4}$, correspondingly).

These calculations demonstrate that only $R_{eff,4}^{(min)}$ is close to the observable value $R_{2t} \sim 3$ Mpc [26]. Calculations for other values of the concentration parameter c from the considered region lead to the same conclusion. Hence, only the marginal value $R_{eff,4}^{(min)}$ corresponds to the observations. We summarize the results of our calculations in Table 1.

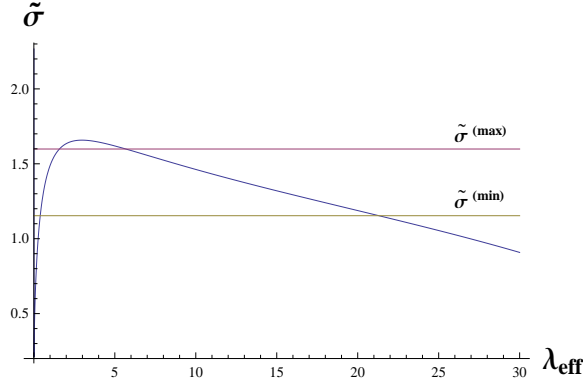


Figure 1. This plot shows the behavior of the dimensionless velocity dispersion $\tilde{\sigma}$ as a function of λ_{eff} for the concentration parameter $c = 4$ (curved line). Upper and lower horizontal lines correspond to the maximal and minimal values of $\tilde{\sigma}$ obtained with the help of the observable data.

This table shows that the closest with respect to the observations results take place for the values $c = 3 \div 4$ where $R_{eff,4}^{(min)}$ has a minimum.

It is worth noting that this concentration parameter is very close to the one obtained from the fitting of the NFW model. This fit is based on a series of DM cosmological simulations within the Λ CDM model [15, 37]. For example, if we take $M_{200}^{(min)} = 1.29h^{-1} \times 10^{15} M_{\odot}$ (see footnote 1), then we get from Eq. (24) in [15] or equivalently Eq. (8) in [37] that $c \approx 3.89$.

Therefore, the comparison of our toy model with the observable data and simulations leads to the following preferable NFW parameters for the Coma cluster: $R_{200} \approx$

$1.77 h^{-1} \text{ Mpc} = 2.61 \text{ Mpc}$ and $c = 3 \div 4$. For these values of c and $M_{200} = 1.29 h^{-1} \times 10^{15} M_{\odot}$, the total mass of the Coma cluster in the case of the NFW profile is $M = (4.08 \div 4.74) h^{-1} \times 10^{15} M_{\odot}$ (see Eq. (3.7)). We also found that in this cluster the most of galaxies are concentrated inside a sphere of the effective radius $R_{eff} \sim 3.7 \text{ Mpc}$ and the line-of-sight velocity dispersion is 1004 km s^{-1} . This value is very close to 1008 km s^{-1} obtained from the observations for the Coma cluster (Abell 1656) in [34].

4 Conclusion

In the present paper we have investigated the distribution of visible and dark matter in the Coma cluster. In the late Universe, such clusters are gravitationally bound systems and can be considered as isolated objects. To study them, we can apply the discrete cosmology (mechanical) approach [18, 19]. In this approach, the motion of a test body in the vicinity of an inhomogeneity is defined by two factors: the gravitating attraction of the inhomogeneity and the accelerated cosmological expansion of the Universe. These two competitive mechanisms define a region where the acceleration of a test body is equal to zero: the zero acceleration surface. In the case of spherical distribution of matter this surface is a sphere of the radius R_H . Inside this sphere, the gravitational attraction plays the main role while at the larger distances the cosmological expansion prevails. This is the region of the Hubble flows formation. It is well known that the DM halo gives the main contribution to the total mass of a cluster. Hence, the gravitational potential of a cluster is mainly defined by the DM distribution in it. There are a number of halo profiles proposed to describe the DM distribution in galaxies and clusters of galaxies. It is natural to define the edge of the DM halo at the radius of zero acceleration. Because the halo of DM dominates in clusters of galaxies, the visible matter in the form of galaxies is considered as test bodies in the gravitational field of the halo.

In our paper, we have investigated the Poisson equation for the gravitational potential of a spherically symmetric halo profile. We have defined the proper boundary conditions at R_H . Then, with the help of the virial theorem, we have got the formula for the mean velocity dispersion for the visible matter (galaxies) inside this halo. Observations show [26] that galaxies inside clusters are abruptly bounded at some distance R_{2t} which is considerably less than the size of the cluster. The most galaxies are inside this distance from the center of mass of the Coma cluster [26]. Since we do not know the real 3D velocities of galaxies, we have supposed a toy model where all galaxies are concentrated inside a sphere of an effective radius R_{eff} with the constant number density. This has enabled us to get the expressions for the mean velocity dispersion for an arbitrary spherically symmetric halo profile.

To perform specific calculations, we need to suggest a definite form for the DM density profile. The NFW profile [35] is one of the most commonly used. We have used this profile in the case of the Coma cluster. First, we have got the formula for the gravitational potential in this profile. Then, we have obtained the mean velocity dispersion as a function of R_{eff} . We have shown that the calculated value of R_{eff} can be rather close to the observable R_{2t} within the observation accuracy of the NFW parameters. Moreover, the comparison of our toy model with the observable data and simulations leads to the following preferable NFW parameters for the Coma cluster: $R_{200} \approx 1.77 \times h^{-1} \text{ Mpc} = 2.61 \text{ Mpc}$, $c = 3 \div 4$ and $M_{200} = 1.29 h^{-1} \times 10^{15} M_{\odot}$. We have also found that in this cluster the most of galaxies are concentrated inside a sphere of the effective radius $R_{eff} \sim 3.7 \text{ Mpc}$, and the line-of-sight velocity dispersion is 1004 km s^{-1} .

Acknowledgements

We would like to thank V.E. Karachentseva for very useful comments. The work of M. Einhorn is supported by NSF CREST award HRD-1345219 and NASA grant NNX09AV07A.

References

- [1] A.G. Riess *et al.*, *Observational Evidence from Supernovae for an Accelerating Universe and a Cosmological Constant*, *Astron. J.* **116** (1998) 1009; arXiv:astro-ph/9805201.
- [2] S. Perlmutter *et al.*, *Measurements of Omega and Lambda from 42 High-Redshift Supernovae*, *Astrophys. J.* **517** (1999) 565; arXiv:astro-ph/9812133.
- [3] D.J. Eisenstein *et al.*, *Detection of the Baryon Acoustic Peak in the Large-Scale Correlation Function of SDSS Luminous Red Galaxies*, *Astrophys. J.* **633** (2005) 560; arXiv:astro-ph/0501171.
- [4] G. Hinshaw *et al.*, *Nine-Year Wilkinson Microwave Anisotropy Probe (WMAP) Observations: Cosmological Parameter Results*, *ApJS* **208** (2013) 19; arXiv:astro-ph/1212.5226.
- [5] P.A.R. Ade *et al.* [Planck Collaboration], *Planck 2013 results. XVI. Cosmological parameters*, *Astron. Astrophys.* **571** (2014) A16; arXiv:astro-ph/1303.5076; P.A.R. Ade *et al.* [Planck Collaboration], *Planck 2015 results. XIII. Cosmological parameters*; arXiv:astro-ph/1502.01589.
- [6] A. Vikhlinin, A. Kravtsov, W. Forman, C. Jones, M. Markevitch, S.S. Murray and L. Van Speybroeck, *Chandra sample of nearby relaxed galaxy clusters: mass, gas fraction, and mass-temperature relation*, *Astrophys. J.* **640** (2006) 691; arXiv:astro-ph/0507092.
- [7] B. Novosyadlyj, V. Pelykh, Yu. Shtanov and A. Zhuk, *Dark Energy: Observational Evidence and Theoretical Models (1st volume of three-volume book "Dark energy and dark matter in the Universe", ed. V. Shulga)*, Akadempriodyka, Kiev (2013); arXiv:astro-ph/1502.04177.
- [8] J. Diemand and B. Moore, *The structure and evolution of cold dark matter halos*, *Advanced Science Letters*, **4** (2011) 297; arXiv:astro-ph/0906.4340.
- [9] V. Lukovic, P. Cabella and N. Vittorio, *Dark Matter in Cosmology*, *Int. J. Mod. Phys. A* **29** (2014) 1443001; arXiv:astro-ph/1411.3556.
- [10] A. Boyarsky, O. Ruchayskiy, D. Iakubovskiy, A.V. Maccio and D. Malyshev, *New evidence for dark matter*; arXiv:astro-ph/0911.1774.
- [11] A. Boyarsky, A. Neronov, O. Ruchayskiy and I. Tkachev, *Universal properties of Dark Matter halos*, *Phys. Rev. Lett.* **104** (2010) 191301; arXiv:astro-ph/0911.3396.
- [12] E.T. Lau, D. Nagai, C. Avestruz, K. Nelson and A. Vikhlinin, *Mass Accretion and its Effects on the Self-Similarity of Gas Profiles in the Outskirts of Galaxy Clusters*, *Astrophys. J.* **806** (2015) 68; arXiv:astro-ph/1411.5361.
- [13] N. Okabe, M. Takada, K. Umetsu, T. Futamase and G.P. Smith, *LoCuSS: Subaru Weak Lensing Study of 30 Galaxy Clusters*, *Publ. Astron. Soc. Jap.* **62** (2010) 811; arXiv:astro-ph/0903.1103.
- [14] A. Saburova and A. Del Popolo, *On the surface density of dark matter haloes*, *Mon. Not. R. Astron. Soc.* **445** (2014) 3512; arXiv:astro-ph/1410.3052.
- [15] M. Schaller *et al.*, *The masses and density profiles of halos in a LCDM galaxy formation simulation*; *Mon. Not. R. Astron. Soc.* **451** (2015) 1247; arXiv:astro-ph/1409.8617.
- [16] L. Chemin, W.J.G. de Blok and G.A. Mamon, *Improved Modeling of the Mass Distribution of Disk Galaxies by the Einasto Halo Model*, *Astron. J.* **142** (2011) 109; arXiv:astro-ph/1109.4247.

- [17] G.S. Bisnovatyi-Kogan and A.D. Chernin, *Dark energy and key physical parameters of clusters of galaxies*, Astrophysics and Space Science **338** (2012) 337; arXiv:astro-ph/1206.1433.
- [18] M. Eingorn and A. Zhuk, *Remarks on mechanical approach to observable Universe*, JCAP **05** (2014) 024; arXiv:astro-ph/1309.4924.
- [19] M. Eingorn and A. Zhuk, *Hubble flows and gravitational potentials in observable Universe*, JCAP **09** (2012) 026; arXiv:astro-ph/1205.2384.
- [20] I. D. Karachentsev *et al.*, *The very local Hubble flow*, Astronomy and Astrophysics **389** (2002) 812; arXiv:astro-ph/0204507.
- [21] I.D. Karachentsev, O.G. Kashibadze, D.I. Makarov and R.B. Tully, *The Hubble flow around the Local Group*, Mon. Not. R. Astron. Soc. **393** (2009) 1265; arXiv:astro-ph/0811.4610.
- [22] I.D. Karachentsev, *Missing dark matter in the local Universe*, Astrophysical Bulletin **67** (2012) 123; arXiv:astro-ph/1204.3377.
- [23] I.D. Karachentsev and O.G. Nasonova, *The observed infall of galaxies towards the Virgo cluster*, Mon. Not. R. Astron. Soc. **405** (2010) 1075; arXiv:astro-ph/1002.2085.
- [24] A. Chernin, P. Teerikorpi and Yu. Baryshev, *Why is the Hubble flow so quiet?*, Adv. Space Res. **31** (2003) 459; arXiv:astro-ph/0012021.
- [25] M. Eingorn, A. Kudinova and A. Zhuk, *Dynamics of astrophysical objects against the cosmological background*, JCAP **04** (2013) 010; arXiv:astro-ph/1211.4045.
- [26] R.B. Tully, *Galaxy Groups*, Astron. J. **149** (2015) 54; arXiv:astro-ph/1411.1511.
- [27] P.J.E. Peebles, *The large-scale structure of the Universe*, Princeton University Press, Princeton (1980).
- [28] V. Springel, *The cosmological simulation code GADGET-2*, Mon. Not. R. Astron. Soc. **364** (2005) 1105; arXiv:astro-ph/0505010.
- [29] A. Melchiorri, L. Pagano and S. Pandolfi, *When Did Cosmic Acceleration Start?*, Phys. Rev. D **76** (2007) 041301; arXiv:astro-ph/0706.1314.
- [30] B. Binggeli, A. Sandage and G.A. Tamman, *Studies of the Virgo cluster. II. A catalog of 2096 galaxies in the Virgo cluster area*, Astron. J. **90** (1985) 1681.
- [31] B. Binggeli, G.A. Tammann and A. Sandage, *Studies of the Virgo cluster. VI. Morphological and kinematical structure of the Virgo cluster*, Astron. J. **94** (1987) 251.
- [32] A. Boselli *et al.*, *The GALEX Ultraviolet Virgo Cluster Survey (GUViCS). IV: The role of the cluster environment on galaxy evolution*, Astronomy & Astrophysics **570** (2014) A69; arXiv:astro-ph/1407.4986.
- [33] T. Sasaki, K. Matsushita, K. Sato and N. Okabe, *Suzaku observations of subhalos in the Coma cluster*; arXiv:astro-ph/1504.03044.
- [34] M.F. Struble and H.J. Rood, *A compilation of redshifts and velocity dispersions for ACO clusters*, Astrophys. J. **125** (1999) 35.
- [35] J.F. Navarro, C.S. Frenk and S.D.M. White, *The structure of Cold Dark Matter Halos*, Astrophys. J. **462** (1996) 563; arXiv:astro-ph/9508025.
- [36] J.M. Kubo *et al.*, *The Mass Of The Coma Cluster From Weak Lensing In The Sloan Digital Sky Survey*, Astrophys. J. **671** (2007) 1466; arXiv:astro-ph/0709.0506.
- [37] A.A. Dutton and A.V. Maccio, *Cold dark matter haloes in the Planck era: evolution of structural parameters for Einasto and NFW profiles*, Mon. Not. R. Astron. Soc. **441** (2014) 3359; arXiv:astro-ph/1402.7073.